Available online at www.sciencedirect.com
ScienceDirect
Journal of Asian Earth Sciences 29 (2007) 84–104
Journal of Asian Earth Sciences
www.elsevier.com/locate/jaes

Paleoenvironmental changes and depositional history of the Korea (Tsushima) Strait since the LGM

Gee Soo Kong [a,*], Soo Chul Park [b]

[a] Petroleum and Marine Resources Division, Korea Institute of Geoscience and Mineral Resources, # 30, Gajeong-dong, Yuseong-gu, Daejeon 305-350, Republic of Korea
[b] Department of Oceanography, Chungnam National University, Daejeon 305-764, Republic of Korea

Received 26 May 2005; received in revised form 16 November 2005; accepted 23 January 2006

Abstract

Two deep cores (SSDP 102 and SSDP 105) from the southeastern inner shelves of Korea were examined in order to reconstruct the paleoenvironmental history of the Korea Strait during postglacial sea-level fluctuations. The results of the lithofaces, organic geochemical components, foraminiferal assemblages, and stable isotopes show that the Korea Strait was influenced in different ways by river discharges and open-ocean currents, according to their temporal and spatial variability.

The results of core SSDP 105 indicate that the southeastern coast of Korea was probably a shallow coastal environment, such as a shoreface or beach, by about 17.5 cal ka. The area remained a coastal environment that was affected by high energy conditions and partly by freshwater input during the transgressive period of 17.5–8.1 cal ka. The area has changed to a modern-type shelf environment influenced by the inflow of the Tsushima Current and by the high supply of fine-grained sediments derived from the Nakdong River since 8.1 cal ka.

Meanwhile, the results of core SSDP 102 taken from the Nakdong River mouth reveal that the river mouth area was most likely a terrestrial or fluvial environment at least before 13.9 cal ka. It then changed to the estuarine (deltaic) environment that was directly affected by the Nakdong River between 13.9 and 7.0 cal ka, and established a modern-type shelf (prodeltaic) environment, which is similar in many respects to the southeastern coast of Korea after temporarily undergoing erosion between 7.0 and 6.1 cal ka.

Keywords: Korea Strait; Tsushima Current; Postglacial paleoenvironmental changes

1. Introduction

During the last glacial maximum (LGM) when global sea-level stood some 120–130 m lower than present (Fairbanks, 1990; Lambeck et al., 2002; Liu et al., 2004), most shelves in the Korea Strait were subaerially exposed. Thus, it was believed that the paleo-Tsushima Current could not have flowed through the Korea Strait into the East/Japan Sea during that time (Oba et al., 1991; Keigwin and Gorbarenko, 1992). However, recent detailed paleogeographic studies, based on detailed radiocarbon dating and the distribution pattern of river-derived lowstand deposits, suggest that the Korea Strait was not closed even during the LGM, so that the paleo-Tsushima Current did flow into the southern part of the East/Japan Sea along a deep, elongated, western channel of the Korea Strait, although its volume transport was much lower than it is today (Park et al., 2000; Lee and Nam, 2003).

The Tsushima Current is characterized by high temperature (14–24 °C) and high salinity (34.6–35‰); not surprisingly, it has a great influence on the regional climate as well as on the hydrodynamic regime (Qin et al., 1996). For these reasons, it is quite significant to

* Corresponding author. Fax: +82 42 862 7275.
E-mail address: kong@kigam.re.kr (G.S. Kong).

1367-9120/$ - see front matter
doi:10.1016/j.jseaes.2006.01.004

know when and how far the Tsushima Current arrived. The Korea Strait has therefore played an important role as a unique pathway for the Tsushima Current that transports heat and salt into the East/Japan Sea.

Although many sedimentological and sequence stratigraphic studies have been carried out in the Korea Strait (Park and Khim, 1990; Park et al., 1999; Kim et al., 2001; Yoo et al., 2003), very few paleoenvironmental studies of the post-LGM have been undertaken. In this study, we describe the chronological, lithological, and organic geochemical results of two deep cores (SSDP 102 and SSDP 105) that were collected from the nearshore off the Nakdong River mouth and along the southeastern coast of Korea, respectively. Based on the results of these studies, we compare and discuss in detail the temporal and special variability of the water mass associated with inflow of the Tsushima Current in order to reconstruct the paleoenvironmental history of the Korea Strait since the LGM.

2. Geological and oceanographic settings

The Korea Strait, which runs between Japan's Kyushu region and the southeastern coast of Korea, is divided into the western and eastern channels by Tsushima Island (Fig. 1). Morphological characteristics of the eastern channel on the Japanese side show a relatively wide and flat seafloor with a depth shallower than 140 m, whereas the western channel on the Korean side is characterized by a narrow, elongated trough as deep as 230 m.

At present, there are discrete surface sediment distributions in the inner, middle, and outer shelves (Fig. 2). The outer shelf, which is deeper than 100 m, is widely overlain by relict sandy mud that was deposited under shoreface complex/beach conditions during the lowstand stage of postglacial sea-levels. The middle shelf has a depth of 100–50 m and is mainly composed of sand deposited during the transgressive stage, whereas the inner shelf is shallower than 50 m and is filled by thick mud deposited

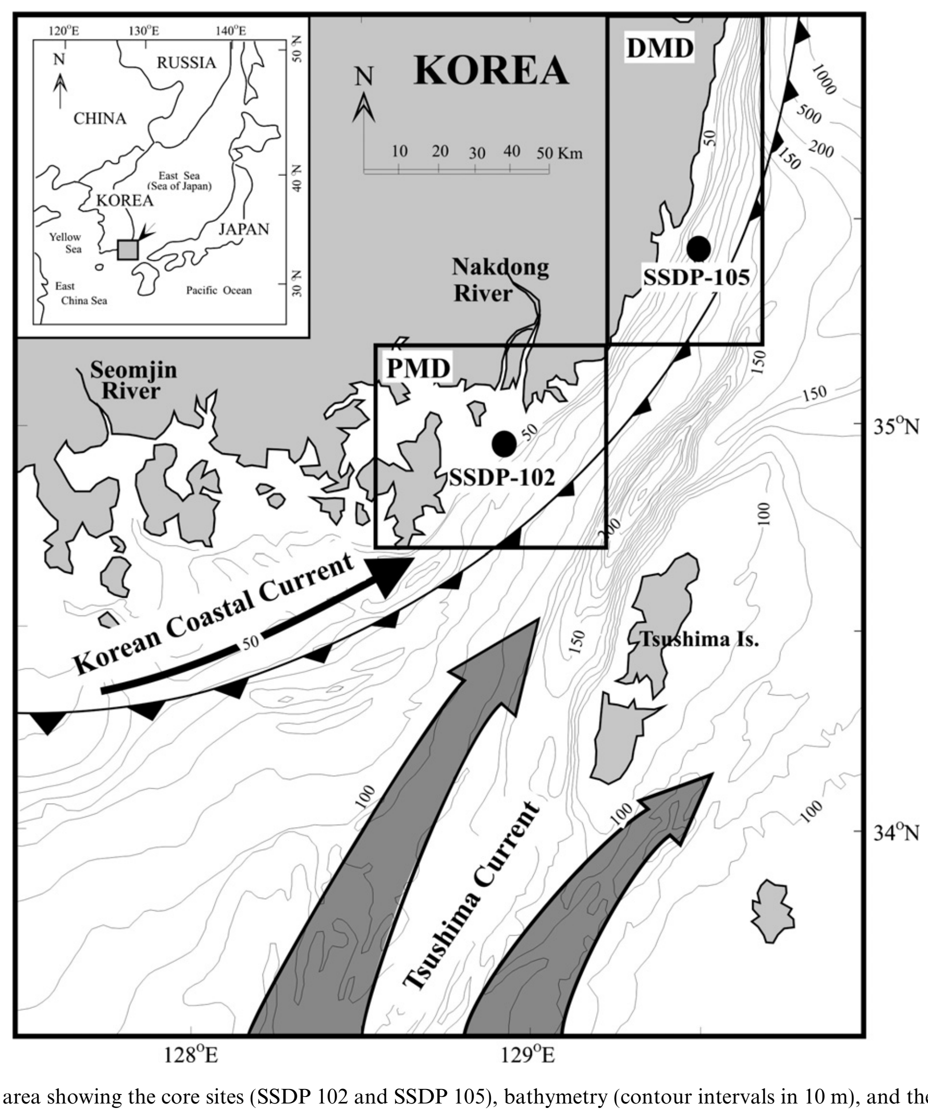

Fig. 1. Map of the study area showing the core sites (SSDP 102 and SSDP 105), bathymetry (contour intervals in 10 m), and the regional current system. The filled triangles indicate a strong coastal front between the Korean Coastal Current and the Tsushima Current.

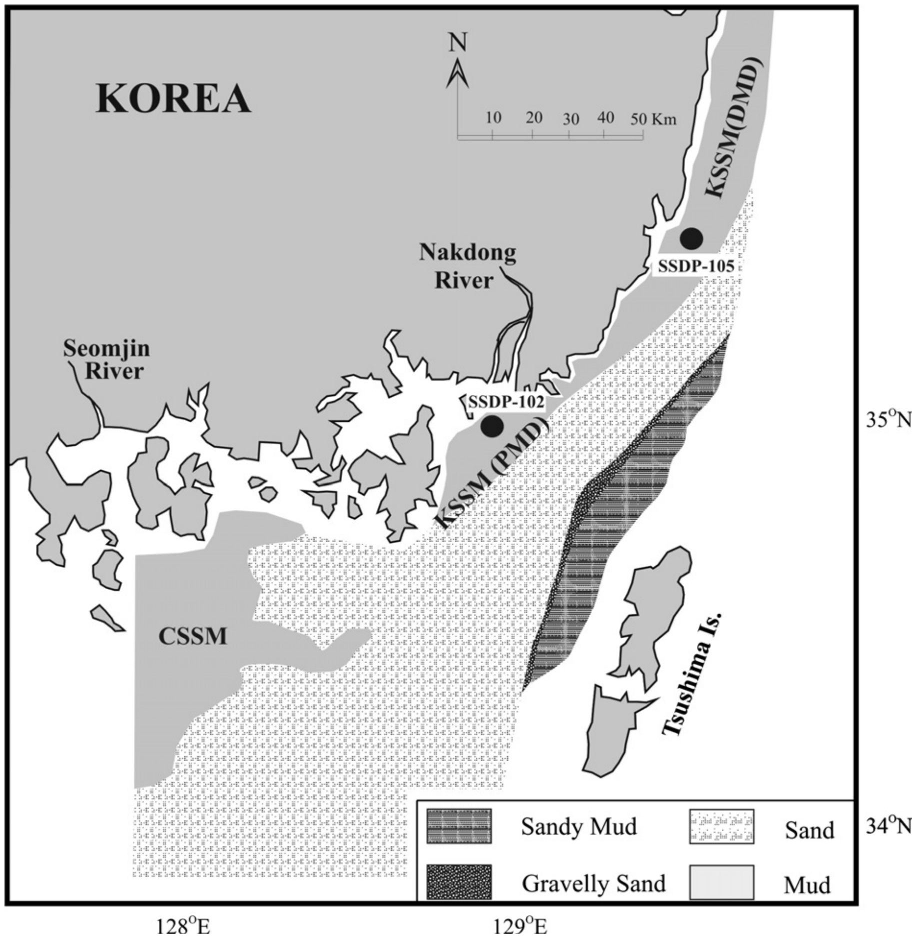

Fig. 2. Surface sediment distributions in the Korea Strait (Yoo et al., 2003). The inner shelf is covered by major recent mud deposits such as the central South Sea mud (CSSM) and the Korea Strait shelf mud (KSSM). The Korea Strait shelf mud (KSSM) along the southeastern coast of Korea is divided into the proximal mud deposits (PMD) and the distal mud deposits (DMD) according to Park et al. (1999).

during the highstand stage (Park et al., 2000; Yoo et al., 2003).

These recent mud deposits, which form the Korea Strait shelf mud (KSSM), originated from a large volume of fine-grained sediments sourced by the Nakdong River (Fig. 2). Based on distribution patterns and acoustic characteristics, the KSSM has been subdivided into two areas: the proximal mud deposits (PMD) off the Nakdong River mouth and the distal mud deposits (DMD) along the southeastern coast of Korea (Park et al., 1999).

At present, the distributions of surface sediments in the western part of the Korea Strait are largely controlled by the tidal currents, the Korean Coastal Current (KCC), and the Tsushima Current. The tidal current flows in a SW–NE direction and causes re-suspension and re-deposition of fine-grained sediments derived from the Nakdong River. The coastal current flows in a NE direction and works as a net transporter of these fine-grained sediments. The strong coastal front between the brackish coastal waters and the saline waters of the Tsushima Current traps the fine-grained sediments, preventing their escape from the nearshore (Park and Chu, 1991; Park et al., 1999). The water–mass properties in the study area are mainly controlled by the saline Tsushima Current waters and by freshwater drained from the Nakdong River (Fig. 1).

3. Materials and methods

Core SSDP 102 (34°57.18′N, 128°52.87′E; core length, 31.6 m; water depth, 40 m) was recovered from an area of proximal mud deposits (PMD) near the Nakdong River mouth by a Chinese drilling vessel (*R/V KAN407*) in 1998. The same vessel obtained core SSDP 105 (35°22.18′N, 129°29.00′E; core length, 51.7 m; water depth, 79 m) in 2000 from an area of distal mud deposits (DMD) along the southeastern coast of Korea.

AMS ^{14}C ages of benthic foraminiferal tests, peaty sediments, and peats from several levels in the two cores were measured at three different institutes (Institute of Geological Nuclear Science, New Zealand; AMS laboratory of Seoul National University, Korea; Leibniz Laboratory of Kiel University, Germany). The CALIB 4.4 program was used to convert radiocarbon ages to calendar ages by applying a marine reservoir correction $\Delta R = 0$ because the regional reservoir effect on radiocarbon dating is not measured in Korean coastal waters (P.J. Reimer, personal communication). The calibration limit of the CALIB 4.4 program for converting calendar ages was assumed to be a linear function according to Bard et al. (1998).

Through general grain size analysis, a residual coarse-grained fraction (grain size $< 4\phi$) was collected using a wet sieve with a 63 μm mesh and was weighed after drying at 50 °C for 48 h. The fine-grained fractions (grain size $> 4\phi$) were separated using a pipette method and were weighed after drying at 50 °C (Galehouse, 1971).

Organic geochemical proxies were measured in 180 samples from core SSDP 102 and in 118 samples from core SSDP 105. The total organic carbon for carbonate-free samples (TOC′) and the total carbon for bulk samples (TC) were measured using the LECO WR-112 carbon analyzer. The total organic carbon for carbonate-free samples (TOC′) and the total carbon for bulk samples (TC) are used to obtain the total organic carbon for bulk sediments (TOC) and calcium carbonates ($CaCO_3$) using the following equations (Stein et al., 1994):

$$\mathrm{TOC}\ (\%) = [100 - (8.333 \times \mathrm{TC})]/[(100/\mathrm{TOC}') - 8.333].$$

$$\mathrm{CaCO_3}\ (\%) = (\mathrm{TC} - \mathrm{TOC}) \times 8.333.$$

The total nitrogen (TN) and total carbon (TC) were measured by the LECO CHN 900, and total sulfur (TS) was measured by the LECO CS-132 analyzer. The ratio of total organic carbon to total nitrogen (C/N), and the ratio of total organic carbon to total sulfur (C/S), are good indicators for evaluating the origin of organic matter in marine sediments. Low C/N (<10) and/or low C/S (<5) generally indicate an abundance of marine organic matter, whereas high C/N (>15) and/or high C/S (>10) indicate the abundance of terrigenous organic matter (Berner and Raiswell, 1984; Stein, 1991).

Rock-Eval pyrolysis was performed to obtain the Hydrogen Index (HI) using the Rock-Eval VI instrument at KIGAM. The HI value is also a valuable indicator for evaluating the origin of organic matter. Less than 100 mgHC/gTOC of HI implies that the TOC in marine sediment is mainly composed of terrigenous organic matter, whereas valves between 200 and 400 mgHC/gTOC indicate that the TOC contains a large amount of marine organic matter (Tissot and Welte, 1984).

The elemental analyzer-isotope ratio mass spectrometer (EA-IRMS) at the Korea Basic Science Institute was used to measure the stable carbon isotopes for organic matter ($\delta^{13}C_{org}$). The analytical precision of the analysis is $\pm 0.2‰$. The $\delta^{13}C_{org}$ value is a common indicator used to check the origin of organic matter. If $\delta^{13}C_{org}$ values are in the range of $-24‰$ to $-27‰$, then a dominance of terrigenous organic matter is likely. In contrast, if values are less than $-24‰$, it indicates the dominance of marine organic matter (Ruttenberg and Goñi, 1997).

4. Results

4.1. Lithology

Core SSDP 102 mainly consists of muddy sediment, except for some gravel and thin sand intervals. On the basis of its lithological features, SSDP 102 is divided into four sediment layers (Fig. 3): a thick gravel layer (Unit IV; 31.6–23.3 m) containing rounded, weathered rock fragments (granite, gneiss, and tuff), a brownish gray sandy mud layer (Unit III; 23.3–15 m) with abundant shell fragments, a dark greenish gray muddy sand layer (Unit II; 15–14 m) with abundant burrows, and a dark greenish gray homogeneous mud layer (Unit I; 14 m – core top) with some burrows and shell fragments.

Core SSDP 105 is characterized by a thick muddy sediment with some coarse-grained sediment layers. It is lithologically divided into five layers (Fig. 3): a yellow green laminated mud layer bounded by peat and charcoal layers (Unit *e*; 51.7–41.7 m), a laminated sandy layer (Unit *d*; 41.7–34.3 m) with some mud balls, a disorganized gravel layer (Unit *c*; 34.3–32 m), a laminated sandy layer (Unit *b*; 32–29.9 m) with some burrows, and a dark greenish gray laminated mud layer (Unit *a*; 29.9 m – core top) with some shell fragments.

4.2. Calendar ages and sedimentation rates

The calendar ages and linear sedimentation rates of cores SSDP 102 and SSDP 105 are shown in Table 1. The age-controlled boundaries of each unit in the two cores are calculated by inter- and extrapolation methods. The results for core SSDP 102 are as follows: Unit IV (>13.9 cal ka), Unit III (13.9–7.0 cal ka), Unit II (7.0–6.1 cal ka), Unit I (6.1 cal ka – present). The average sedimentation rates, when plotted against calendar ages in core SSDP 102, are 0.9 m/kyr in Unit III and 2.8 m/kyr in Unit I (Fig. 4). The sedimentation rate of Unit II is ignored because it corresponds to the erosional surface as identified in 3.5 kHz seismic profiles (KIGAM, 2000).

In core SSDP 105, the upper boundary of Unit *e* is overlain by peat (41.7 m) and is dated to be 53.7 cal ka. The boundaries of Unit *d* and Unit *c* were not estimated because of the likelihood of unconformities. The lower boundary of sand-dominated Unit *b* is estimated to be approximately 17.5 cal ka (15,080 ^{14}C year BP), which is based on the suggestion that the gravel-dominated Unit *c* is well correlated to the relict sediments on the outer shelf of the Korea Strait (Yoo and Park, 1997). The lower boundary of mud-dominated Unit *a* is extrapolated to be 8.1 cal ka. The sedimentation rates of Unit *a* clearly increase upward with an average of 6.7 m/kyr (Fig. 4).

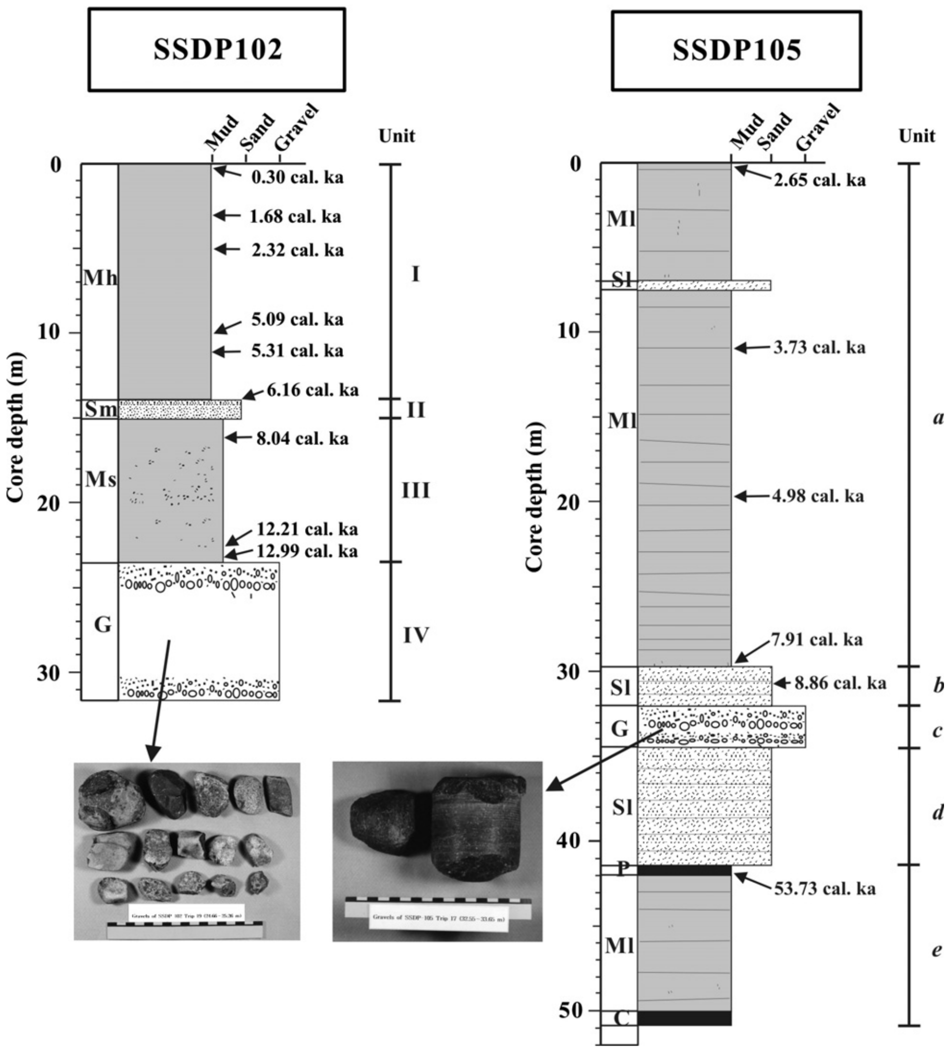

Fig. 3. Lithology, calendar ages, and depositional units in core SSDP 102 and SSDP 105 (Mh, homogenous Mud; Ml, laminated Mud; Ms, sandy Mud; Sl, laminated Sand; Sm, muddy Sand; G, Gravel; P, Peat; C, Charcoal). The photos represent the gravels recovered at the bottom of core SSDP 102 and those at core depths of 32–34 m of core SSDP 105, respectively.

4.3. Coarse fractions, $CaCO_3$ contents, and organic geochemical components

The results of tests on core SSDP 102 are summarized in Appendices A and B. Coarse fractions (grain size < 4ϕ) show a wide range of between 96.8% and 5.2% (Fig. 5). In Unit III, they decrease rapidly to 6.2%, and then slightly increase up to 36.5%. In Unit II, they increase drastically up to 72%. In Unit I, however, they remain less than 5.2% after abruptly decreasing. $CaCO_3$ contents are not as widely variable as coarse fractions. In Unit III, they sustain low values of less than 5% (avg. 2.6%) with little variation. In Unit II, they increase suddenly to 17.7%. In Unit I, they decrease gradually from 15% to 5% (avg. 9.7%). TOC values in Unit III fluctuate between 0.1% and 1.1% and then decrease abruptly to less than 0.5% in Unit II. In Unit I, however, they sustain high values of more than 1% after distinctively increasing. C/N ratios range from 2.0 to 14.2. In Unit III, they are above 10 and vary significantly. In Unit II, the ratios decrease to less than 10. In Unit I, they gradually increase from 5 to 10, but most do not exceed 10. C/S ratios do not show a good correlation with other organic geochemical proxies: <2 in Unit III, 0.7–43 in Unit II, and 2–13 in Unit I. Most of the $\delta^{13}C_{org}$ values (‰) are less than −24‰ in Unit III, but increase rapidly in the lower boundary of Unit II and maintain a level of more than −22‰ in Unit I. HI values in Unit I are slightly higher than those in other units, even though they are still less than 100 mgHC/gTOC.

The results of core SSDP 105 are shown in Appendices C and D. Coarse fractions show high values between 60% and 87.5% in Unit *b* but remain less than 10% (avg. 4.2%) in Unit *a* after rapidly decreasing (Fig. 5). $CaCO_3$ contents show low values, between 2.7% and 7.5%, in Unit *b*, but increase sharply to about 15% in Unit *a*. TOC values show low values, between 0.08 and 0.54%, in Unit *b*, but increase abruptly to about 2.0% in Unit *a*. C/N ratios show less than 5 in Unit *b*, whereas they show between 5 and 10 in

Table 1
Ages and average sedimentation rates in cores SSDP102 and SSDP 105

Core No.	Depth (m)	AMS ^{14}C age (yr BP)	Calendar age (cal yr)	Sedimentation rate (m/kyr)	Materials	Laboratory Ref. No.
SSDP102	0.47	682 ± 60	304	1.5	Bulk benthic Foram	KIA19445
SSDP102	3.05	2,090 ± 25	1,680	1.9	Bulk benthic Foram	KIA19446
SSDP102	5.09	2,630 ± 20	2,315	3.2	Bulk benthic Foram	KIA19447
SSDP102	10.50	4,830 ± 50	5,094	1.9	Bulk benthic Foram	KIA19448
SSDP102	11.25	4,990 ± 30	5,310	3.5	Bulk benthic Foram	KIA19449
SSDP102	14.05	5,715 ± 81	6,157	3.3	*Lenticulina calcar* (Linn'e)	NZA10040
SSDP102	16.23	7,610 ± 55	8,036	1.2	Bulk benthic Foram	NZA10041
SSDP102	22.93	10,858 ± 80	12,206	1.6	Bulk benthic Foram	NZA10042
SSDP102	23.10	11,474 ± 60	12,991	0.2	Peaty sediment	NZA10757
SSDP105	0.60	2,835 ± 45	2,652	0.2	Bulk articulated shell	NZA15761
SSDP105	10.99	3,805 ± 40	3,725	9.7	Bulk benthic Foram	KIA21880
SSDP105	19.90	4,755 ± 65	4,978	7.1	Bulk benthic Foram	NZA15757
SSDP105	29.72	7,445 ± 45	7,914	3.3	Bulk benthic Foram	KIA21881
SSDP105	30.89	8,325 ± 45	8,861	1.2	Bulk benthic Foram	KIA21883
SSDP105	41.70	46,000 ± 2000	53,728	0.2	Peat	SNU00-379

KIA denotes the laboratory number for the Leibniz Laboratory at Kiel University, NZA refers to the Institute of Geological Nuclear Science (IGNS), and SNU is the AMS laboratory at Seoul National University.

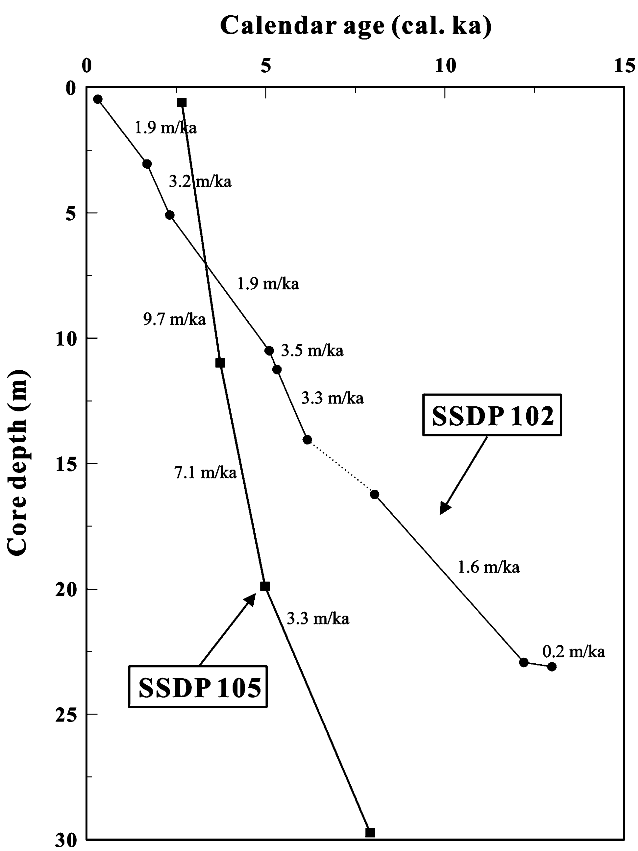

Fig. 4. Average sedimentation rates plotted against calendar ages in core SSDP 102 and core SSDP 105. Dashed line in SSDP 102 shows the interval of the embedded sand layer corresponding to the erosional boundary as identified in 3.5 kHz seismic profiles (KIGAM, 2000).

Unit I. C/S ratios are under 3 in Unit *b*, but increase to more than 3 in Unit *a*. $\delta^{13}C_{org}$ values show low values, between −25.5‰ and −22.4‰, in Unit *b*, but increase to over −22.0% in Unit *a*. Most HI values are lower than 100 mgHC/gTOC in Unit *b*, whereas they show high values within a wide range of 100–500 mgHC/gTOC in Unit *a*.

5. Discussion

The results from the two deep core samples (SSDP 102 and SSDP 105) suggest that the inner shelves of the Korea Strait have evolved from fluvial or shoreface environments to a modern-type shelf environment since the LGM probably primarily because of rising sea-levels, and second because of the inflow of an oceanic current. The results also reveal that the distributions of the recent mud deposits (KSSM; PMD and DMD) in the inner shelves of the Korea Strait are largely related to such paleoenvironmental changes.

5.1. The lowstand stage of sea-level

In core SSDP 105, taken from the southeastern coast of Korea, coarse gravels (>10 cm in diameter) were recovered at core depths of 34–32 m (Unit *c*) and are assumed to be relict sediments deposited at the lowstand stage. Yoo and Park (1997) suggested that relict sediments presently remain at a depth of 120–150 m in the outer shelf of the Korea Strait and that they were formed at around 17.5 cal ka (15.0 ^{14}C ka). Park et al. (2000) also proposed that these relict sediments were deposited within beach/shoreface environments during the lowstand stage. The paleo-water depth of the deposited coarse gravels in core SSDP 105 may be estimated by adding the present water depth (79 m) to the sampling depth of the gravels (34–32 m). The calculated depth (approximately 112 m) is very close to the global sea-level position at around 17.5 cal ka (Fairbanks, 1990; Lambeck et al., 2002), assuming that no vertical isostatic and/or tectonic movement occurred near the Korea Strait since deposition. As shown

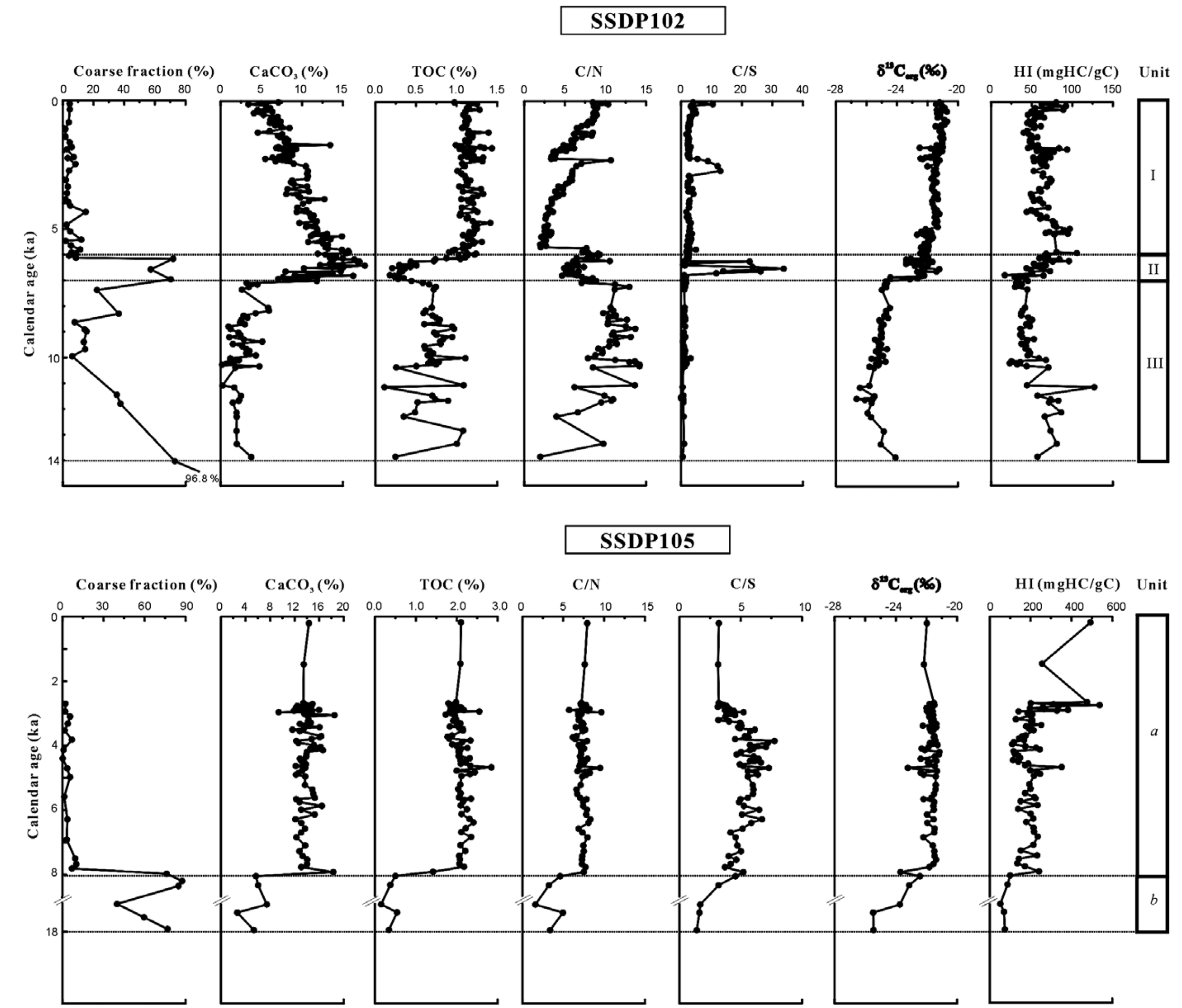

Fig. 5. Vertical variations of coarse fraction (%), calcium carbonate (%), total organic carbon (%), C/N ratio, C/S ratio, carbon isotope for organic matter (‰), and hydrogen index (mgHC/gTOC) in cores SSDP 102 and SSDP 105, respectively.

in Fig. 3, these coarse gravels are composed of well-rounded trachyte fragments and are lithologically similar to relict sediments in the outer shelf (Yoo et al., 2003). These results suggest that the southeastern coastal area was probably a shoreface environment at least by 17.5 cal ka.

In core SSDP 102, collected near the Nakdong River mouth area, the upper boundary of a thick gravel layer (31.6–23.3 m; Unit IV) was calculated to be 13.9 cal ka (Fig. 3). Fairbanks's (1990) sea-level curve predicts that sea-level at that time was 95 m lower than its present level. Considering both the present water depth (40 m) at the core SSDP 102 site and the upper sampling depth of the gravel (23.3 m), it can be presumed that these gravels were deposited under non-marine conditions. As shown in Fig. 3, these gravels are composed of oxidized/well-rounded sedimentary and volcanic rock fragments (granite, gneiss, and tuff). Yoo and Park (1997) have suggested that the paleo-Nakdong River channel developed close to the core SSDP 102 site during this period. Also, the proximity of the core SSDP 102 site to the Nakdong River mouth supports the idea that the study area off the Nakdong River mouth was probably within a fluvial environment before 13.9 cal ka.

5.2. The transgressive stage of sea-level

During the period of 17.5–8.1 cal ka, global sea-level was 110–20 m lower than present. According to findings from core SSDP 105, laminated sand (Unit *b*; 32–29.9 m) was predominant during this period. The persistence of a thin sand layer indicates that the southeastern coastal area was probably hydrodynamically under an active coastal environment and/or rarely received fine-grained sediments from adjacent rivers.

During the early stages of this period, shallow erosion may have occurred in the southeastern coastal area, resulting in deposition of coarse sediment. Also, fine-grained sediments discharged from the paleo-Nakdong River did not reach the southeastern coast of Korea because the paleo-Nakdong River mouth at that time was connected to the deep trough of the outer shelf (Fig. 1). Even during the late stages of this period when sea-level approached its present level, our results show high coarse fractions and simultaneously low TOC contents (Fig. 5), which indicates that the southeastern coastal area was continuously undergoing active erosion.

In general, such a condition results in limited deposition of fine-grained sediments due to the influence of strong wave action, even though the fine-grained sediments were transported by coastal current. Also, deposition of fine sediments in the area was hindered because the strong coastal front between brackish waters and the Tsushima Current was not established at that time. At present, the strong coastal front plays a significant role in trapping fine-grained sediments and prevents their escape to the outer-shelf. According to Yoo and Park (2000), most of the fine-grained sediments from the Nakdong River during this period were preferentially deposited near the Nakdong River mouth because the depositional capacity generated by a sea-level rise outpaced the sediment supply of the Nakdong River.

During the period of 17.5–8.1 cal ka, however, organic geochemical results (e.g., $<-24‰$ of $\delta^{13}C_{org}$ and <100 mgHC/gTOC of HI) reveal that terrigenous organic matter was dominant in the southeastern coastal area, even though the C/N and C/S ratios are not well correlated. These results indicate that the southeastern coastal area was to some extent influenced by river runoff during this transgressive period. This was probably because the paleo-Nakdong River mouth retreated from the outer shelf margin to near its present position due to the rapid increase of water depth. As a result, freshwater derived from the paleo-Nakdong River approached the southeastern coastal area.

In the sandy mud layer (Unit III; 23.3–15 m) overlying the thick gravel layer of core SSDP 102, coarse fractions decrease upward, indicating that the Nakdong River mouth area began to change gradually into a major depocenter of fine-grained sediments derived from the Nakdong River between 13.9 and 7.0 cal ka. During this period, organic geochemical results, such as low $CaCO_3$ contents (<5%), high C/N ratios (>10), low $\delta^{13}C_{org}$ values ($<-22‰$), and mostly low HI values (<50 mgHC/gC), reveal that the Nakdong River mouth area was an estuarine environment that was occupied mainly by terrigenous organic matter. This idea is further supported by benthic foraminifera, such as *Textularia sagittula* and *Ammonia beccarii*, that are prevalent in the brackish environment, and by the absence of typical planktonic foraminifera such as *Globigerinoides ruber* (d'Orbigny) and *Neogloboquadrina dutertrei* (d'Orbigny), which indicates the influence of warm, saline water (Be′, 1977) (Fig. 6).

During the short period from 7.0 to 6.1 cal ka, corresponding to Unit II (15–14 m) of core SSDP 102, a thin sand layer appeared between two thick mud layers, indicating that the Nakdong River mouth area was probably influenced by high energy conditions. This thin sand layer is well correlated to the erosional surface boundary in 3.5 kHz seismic profiles (KIGAM, 2000). It is reported that a similar erosional surface boundary also formed in the southeastern Yellow Sea mud (SEYSM) during the same period (Jin and Chough, 1998). Also, Park et al. (1999) interpreted this erosional boundary as being the transgressive sand layer that formed during the Holocene transgression stage. Previous studies have identified the same type of seismic reflectors in several places near the Nakdong River mouth (Park and Yoo, 1988; Park et al., 1996). This erosional boundary, however, is not observed in other major recent mud deposits overlying the inner shelf of Korean seas, such as the central South Sea mud (CSSM) and the distal mud deposits (DMD) along the southeastern coast (Fig. 2).

5.3. The highstand stage of sea-level

Following the marine transgression, large amounts of fine-grained sediments derived from the Nakdong River may have been deposited in the inner shelf of the Korea Strait to form recent mud deposits (KSSM). Park et al. (1999) proposed that about 35% of the fine-grained sediments that originated from the Nakdong River are deposited near the present river mouth (PMD), whereas the remaining 63% are transported along the southeastern coast of Korea to form shelf-parallel mud deposits (DMD). These recent mud deposits become thinner toward the outer shelf and are ultimately laterally bordered by coarse-grained sediments at water depths of 70–100 m. These recent mud deposits began to form at approximately 6.4 cal ka (6.0 ^{14}C kyr BP), when sea-level reached close to its present level (Suk, 1989; Min, 1994; Park et al., 1996). Our age-controlled lithological results (Unit *a*; 29.9 m – core top) of core SSDP 105, however, indicate that fine-grained sediments derived from the Nakdong River did not begin to be deposited in the southeastern coast (DMD) of Korea until 8.1 cal ka (Fig. 5).

Park and Chu (1991) suggested that most suspended sediments derived from the Nakdong River are dispersed along the coast and accumulate in the nearshore as a result of the combined influence of coastal and tidal currents. In addition, Park et al. (1999) suggested that because of the strong front between coastal waters and offshore Tsushima Current, most fine-grained sediments derived from the Nakdong River mouth are trapped in the nearshore and do not effectively escape the shelf. The development of a 30-m thick mud layer from 8.1 cal ka – present may indicate that oceanic circulation

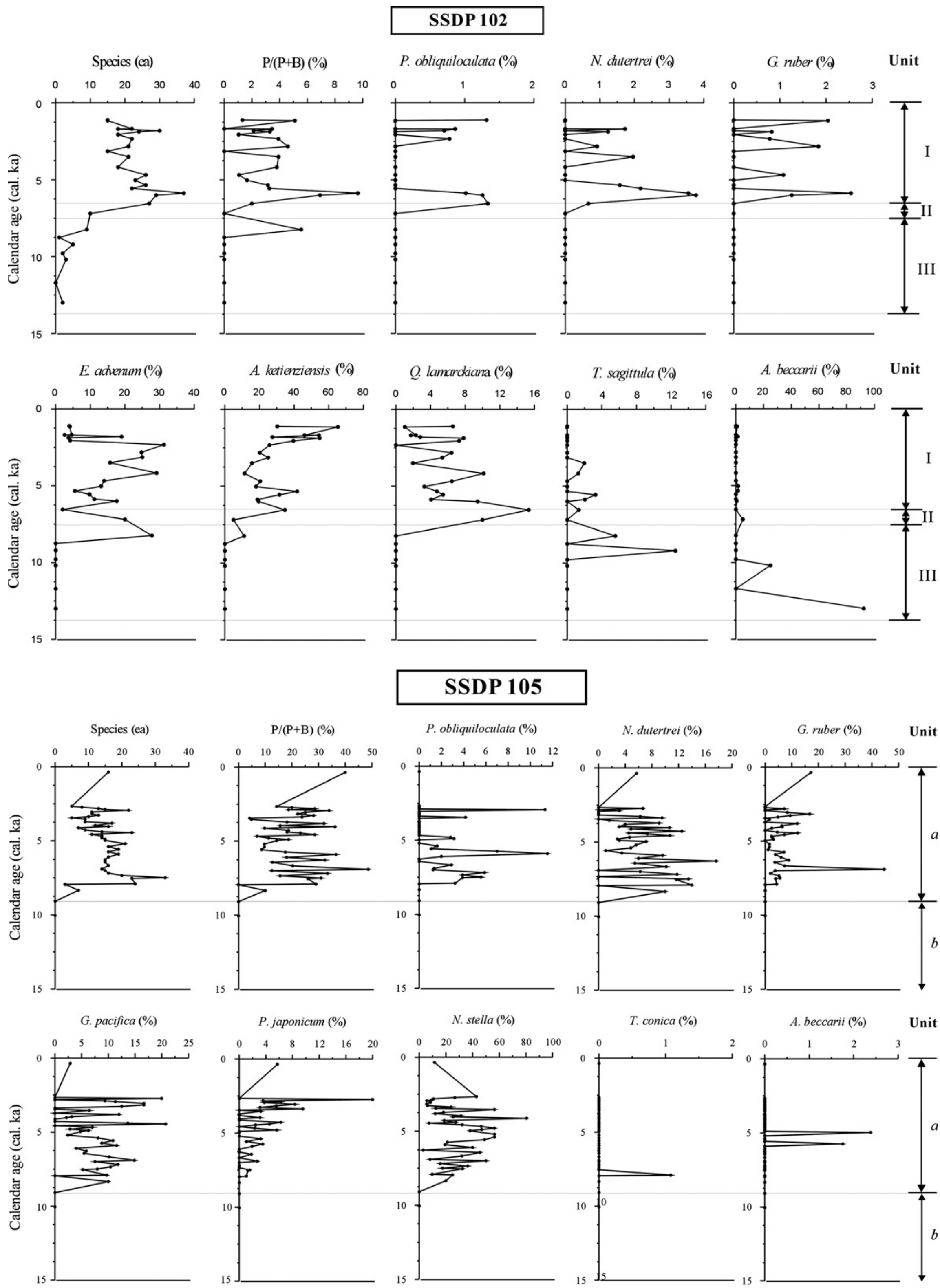

Fig. 6. Vertical occurrences of total foraminiferal species, planktonic/benthic ratio (%), and most common planktonic and benthic foraminiferal species in cores SSDP 102 and SSDP 105, respectively (KIGAM, 2000).

patterns similar to those at present were already established in the inner shelves of the Korea Strait by 8.1 cal ka. In other words, the evolution of a strong coastal front along the southeastern coast suggests that the Tsushima Current had already arrived by that time and affected the southeastern coastal (DMD) area.

Various geochemical proxies are available to provide notable records associated with the inflow of the Tsushima Current. In general, biogenic calcium carbonate in marine sediment is controlled by water–mass properties, biological productivity, water depth, sedimentation, preservation, and dissolution (Anderson, 1975; Kellogg, 1976; Steinsund and Hald, 1994). For the period 8.1 cal ka – present, $CaCO_3$ contents of core SSDP 105 display continuously high values, between 12% and 16% (Fig. 5), indicating that the above controlling factors were mostly maintained during this period. In other words, marine conditions similar to those at present were prevalent in the southeastern coast of Korea since 8.1 cal ka.

Together with an increase in $CaCO_3$ contents, TOC content also shows consistently high values of about 2.0% during the same period (Fig. 5). Also, relatively low C/N ratios (5–10), low C/S ratios (avg. 5), high $\delta^{13}C_{org}$ values ($-23‰$ to $-21‰$), and high HI values (>200 mgHC/gTOC) in core SSDP 105 indicate that such high TOC contents can be attributed to an increase in primary productivity. Knies and Stein (1998) suggested that the increase in marine organic matter by primary productivity, especially in marginal seas, could be caused by the inflow of an open-ocean current.

The idea of an open-ocean current inflow is also supported by evidence of faunal changes in planktonic and benthic foraminiferal species. Typical open-ocean current species of planktonic foraminifera, such as *Pulleniatina obliquiloculata*, *Neogloboquadrina dutertrei*, and *Globigerinoides ruber*, are predominant along the path of the Kuroshio Current in the northwestern Pacific (Be′, 1977). In addition to typical planktonic foraminiferal species, open-oceanic benthic foraminiferal species, such as *Nonionella stella*, *Globobulimina pacifica*, and *Pseudononion japonicum* also become abundant in core SSDP 105 after 8.1 cal ka, whereas brackish benthic foraminiferal species such as *Ammonia beccarii* and *Textularia conica* are almost totally absent. Also, $P/(P + B)$ ratios are 10 times higher than those in core SSDP 102 (Fig. 6).

The major open-ocean current in the northwestern Pacific is the Kuroshio Current which transports a large amount of heat and salt to marginal seas such as the East China Sea, the East/Japan Sea and the Yellow Sea. Although there are different opinions regarding the timing of re-entry of the Kuroshio Current (Jian et al., 2000; Kawahata et al., 2003), it is generally accepted that the Kuroshio Current began to affect marine environments of the marginal seas since early Holocene time. Oba et al. (1991) suggest that the paleo-Tsushima Current, as a branch of the Kuroshio Current, started to flow through the Korea Strait into the East/Japan Sea at 11 cal ka. However, the modern oceanographic regime in the East/Japan Sea was not established until 8.4 cal ka. Xu and Oda (1999) also propose that the Kuroshio Current began to affect the East China Sea in 10.5 cal ka. Ijiri et al. (2005) suggest that the East China Sea changed to the present warm Kuroshio Current condition after 8 ka. These suggestions support the idea that the southeastern coast of Korea began to change into a modern shelf environment by about 8.1 cal ka, when the East/Japan Sea was fully developed by the successive influence of the Tsushima Current.

Meanwhile, the Nakdong River mouth (PMD) area did not change to a modern shelf environment until 6.1 cal ka. Unit I (14 m – top) of core SSDP 102, corresponding to the period of 6.1 cal ka – present, is characterized by high TOC contents derived from an increase in marine organic matter, as supported by organic geochemical results (>5% of $CaCO_3$, >1% of TOC, <10 of C/N ratios, and $>-22‰$ of $\delta^{13}C_{org}$). Such a predominance of marine organic matter suggests that primary productivity increased in core SSDP 102 site since 6.1 cal ka. The fluvial nutrient supply from the Nakdong River could also have induced the increase in primary productivity because the PMD area is still located close to the Nakdong River. Incidentally, the fluvial supply most likely plays a minor role in the increase in primary productivity compared to its role during the transgressive period because the core SSDP 102 site moved further away from the river mouth as sea-level rapidly rose. Accordingly, as above mentioned, such active primary productivity in a marginal sea is primarily caused by the inflow of an open-ocean current.

As shown in Fig. 6, typical planktonic foraminiferal species such as *P. obliquiloculata*, *N. dutertrei*, and *G. ruber* in core SSDP 102 have distinctly increased since 6.1 cal ka, indicating the influence of the Tsushima Current. Additionally, saline benthic foraminifera such as *Elphidium advenum*, *Ammonia ketienziensis*, and *Quinqueloculina lamarckiana* (Wang et al., 1985) increased remarkably in core SSDP 102. Even though the $P/(P + B)$ ratios and occurrences of typical species (%) in core SSDP 102 are lower than those in core SSDP 105, these results show that the marine environment of the Nakdong River mouth (PMD) area was also influenced by the Tsushima Current since 6.1 cal ka, even though the modern shelf condition of the Nakdong River mouth area seems to be slightly different from that of the southeastern coastal area due to the proximity of the Nakdong River.

Compared with the timing in the southeastern coast of Korea, this result indicates that the Tsushima Current lately has significantly intruded into the Nakdong River mouth area. Such a long time lag between two core sites seems to be attributed to the difference in water depth and proximity to the river mouth. According to our results, the altitude of the Nakdong River mouth (PMD) area is higher than the southeastern coast (DMD) area by 48 m. Also, the DMD area is not directly affected by freshwater that is transported by the Korean Coastal Current. Since the highstand stage of sea-level, the Tsushima Current approached the Nakdong River mouth (PMD) area and the current changed the estuarine environment into a modern shelf.

Fig. 7 shows a summary schematic diagram of the paleo-environmental changes in the inner shelves of the Korea

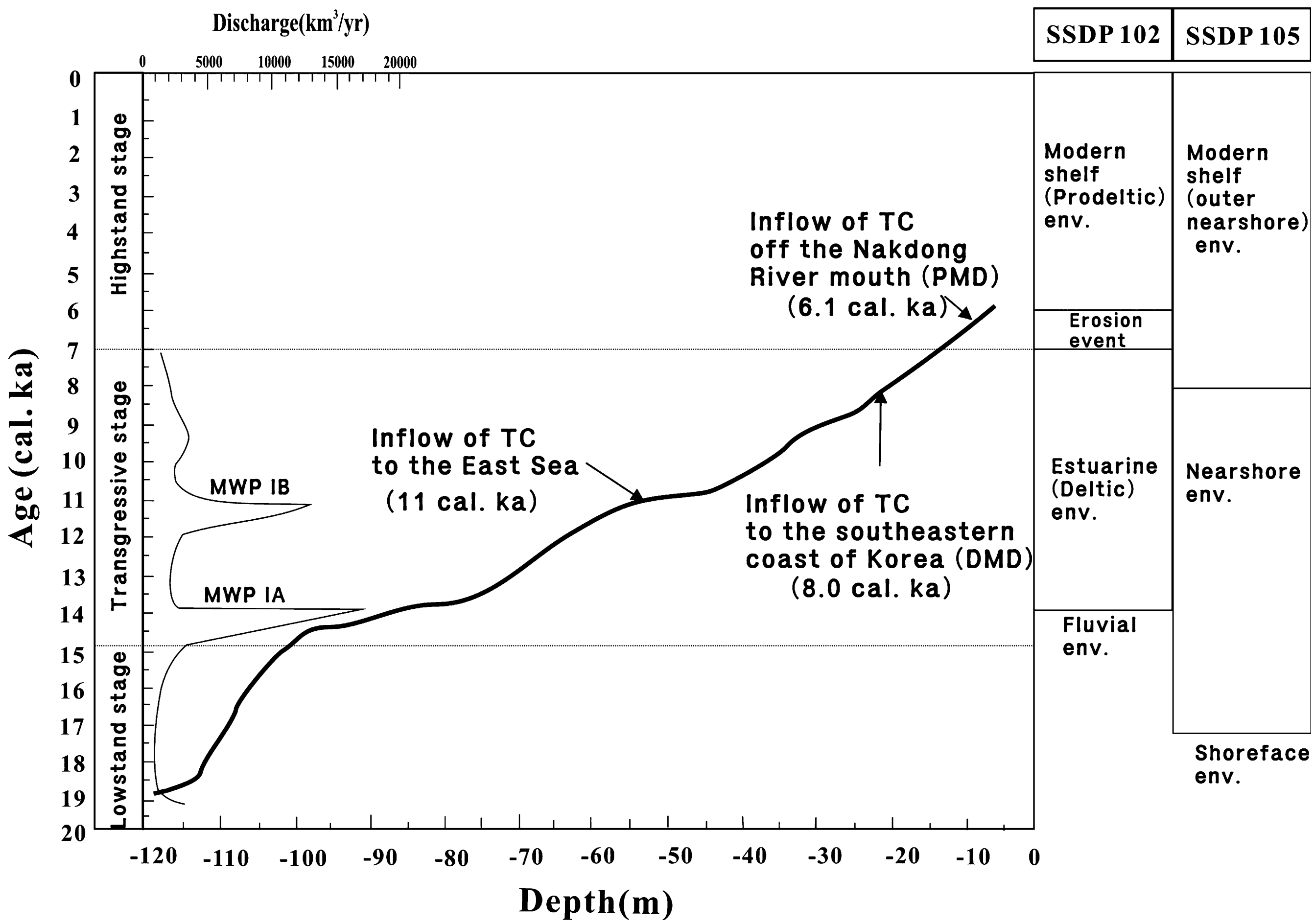

Fig. 7. Summary schematic diagram of the paleoenvironmental changes in the Korea Strait since the LGM. Solid line shows the global sea-level curve based on a Th/U age (Fairbanks, 1990). MWP denotes meltwater pulse and TC indicates the Tsushima Current. The boundary of the sea-level stage is inferred based on the rate of glacial meltwater discharges.

Strait since 17.5 cal ka. Fairbanks (1990) proposed that sea-level rose from −95 to −80 m at MWP 1A (14.3–14.1 cal ka), and soon after from −58 to −43 m at MWP 1B (11.6–11.3 cal ka). By the end of MWP 1A, most of the Korea Strait shelf was probably rapidly submerged; in contrast, however, the Nakdong River mouth (PMD) area was not submerged due to its higher altitude. Such a rapid increase of water depth could make the East/Japan Sea fully connected with the open-ocean. In spite of the rapid rise in sea-level, however, the paleo-Tsushima Current did not begin to flow into the entire East/Japan Sea until the end of the MWP 1B (Oba et al., 1991). During the transgressive stage, which included two major meltwater pulses, the Nakdong River mouth (PMD) area changed from a fluvial (terrestrial) to estuarine (deltaic) environment, whereas the southeastern coast (DMD) area remained a nearshore environment.

6. Conclusions

High-resolution paleoenvironmental records from approximately 17.5 cal ka were obtained from two deep core samples (SSDP 102 and SSDP 105) that were taken from recent mud deposits in the Korea Strait (PMD and DMD). The detailed paleoenvironmental histories of the inner shelves of the Korea Strait are determined from several proxies as follows:

(1) During the lowstand stage, large subrounded gravels occurred in Unit *c* of core SSDP 105, which was taken from the southeastern coast of Korea. These gravels are well correlated with relict sediments in the outer shelf of the Korea Strait that were deposited during the LGM. Considering that the paleo-water depth at Unit *c* is estimated to be 112 m less than the present level, the occurrence of this gravel indicates that the southeastern coastal area was within a shoreface environment by 17.5 cal ka.

Before 13.9 cal ka, the Nakdong River mouth area was filled by strongly oxidized and well-rounded rock fragments (corresponding to Unit IV of core SSDP 102). The inferred paleo-water depth was approximately 32 m higher than sea-level at that time, which indicates that the gravels were probably deposited within a fluvial environment.

(2) During the transgressive stage, the southeastern coastal area was thinly covered by laminated sand with relatively low TOC content and large proportions of terrigenous organic matter (corresponding to Unit *b* in core SSDP 105). These results suggest that the southeastern coastal area was a nearshore environment between 17.5 and 8.1 cal ka, which was partially influenced by freshwater but rarely received fine-grained sediments derived from the Nakdong River.

Between 13.9 and 7.0 cal ka, characteristics of the Nakdong River mouth area included an upward decrease in coarse fractions, large amounts of brackish benthic foraminifera, an absence of planktonic foraminifera, and a predominance of terrigenous organic matter (corresponding to Unit III of core SSDP 102). These results suggest that the Nakdong River mouth area was an estuarine (deltaic) environment directly influenced by the Nakdong River. Between 7.0 and 6.1 cal ka, the embedded sand layer (Unit II) of core SSDP 102 indicates that the area temporarily experienced erosion that was probably caused by a deceleration in the rate of sea-level rise.

(3) During the highstand stage, the southeastern coastal area was characterized by a large amount of fine-grained sediments discharged from the Nakdong River, a large increase in $CaCO_3$ content due to biological activity, a large increase in TOC content due to primary productivity, and a predominance of typical planktonic foraminifera (Unit *a* in core SSDP 105). These characteristics suggest that a modern-type shelf environment began to form in the southeastern coast of Korea by 8.1 cal ka.

Since 6.1 cal ka, which corresponds to Unit I in core SSDP 102, a modern-type shelf (prodeltic) environment in the Nakdong River mouth area was established, as evidenced by a large amount of fine-grained sediments, a relative abundance of marine organic matter, and the occurrence of typical planktonic foraminifera, all of which indicate the continuing influence of the Tsushima Current.

Acknowledgments

We are grateful to Prof. Scourse and another anonymous reviewer whose critical reviews of the manuscript greatly improved its accuracy and clarity. Dr. H.C. Han, Dr. J.H. Chang, Mr. H.J. Kim, and Dr. H.Y. Lee gave many helpful suggestions. This research was supported financially by the Korea Institute of Geoscience and Mineral Resources (KIGAM), and also partly supported by the Basic Research Program of the Korea Science and Engineering Foundation (Grant No. R05-2002-000-00077-0).

Appendix A. Organic geochemical results of core SSDP 102

Depth (m)	Age (cal ka)	$CaCO_3$ (%)	TOC (%)	TN (%)	TS (%)	C/N ratio	C/S ratio	$\delta^{13}C_{org}$ (‰)	HI (mgHC/gC)
0.02	0.01	7.08	0.97	0.11	0.25	8.46	3.93	−21.22	80
0.13	0.08	3.41	1.25	0.12	0.12	10.34	10.41	−21.43	62
0.24	0.16	5.57	1.15	0.13	0.36	8.57	3.20	−21.05	92
0.35	0.23	6.06	1.13	0.13	0.32	8.99	3.51	−20.88	54
0.47	0.30	4.52	1.28	0.15	0.28	8.80	4.56	−21.39	89
0.60	0.37	6.34	1.11	0.13	0.28	8.74	4.02	−20.73	50
0.72	0.44	4.08	1.10	0.13	0.23	8.52	4.90	−21.37	62
0.84	0.50	5.27	1.08	0.12	0.29	8.94	3.78	−21.18	45
0.97	0.57	6.98	1.11	0.13	0.40	8.69	2.80	−21.27	60
1.04	0.61	6.43	1.14	0.13	0.35	8.46	3.23	−21.34	65
1.20	0.69	6.11	1.15	0.13	0.40	8.57	2.89	−20.89	53
1.32	0.76	7.36	1.11	0.14	0.38	7.93	2.95	−20.72	47
1.44	0.82	6.05	1.12	0.13	0.44	8.35	2.57	−20.84	45
1.55	0.88	6.97	1.12	0.15	0.37	7.63	3.00	−20.89	49
1.60	0.91	6.68	1.11	0.14	0.43	7.76	2.58	−21.10	53
1.67	0.94	7.40	1.09	0.16	0.47	7.06	2.31	−21.48	61
1.80	1.01	8.45	1.07	0.16	0.45	6.48	2.39	−21.12	53
2.02	1.13	6.02	1.15	0.17	0.46	6.59	2.49	−21.21	44
2.14	1.19	4.56	1.39	0.16		8.45		−21.05	40
2.25	1.25	7.55	1.14	0.19	0.67	6.13	1.71	−21.00	47
2.37	1.32	7.04	1.19	0.14	0.53	8.31	2.25	−21.10	49
2.48	1.38	7.32	1.19	0.17	0.51	7.12	2.33	−21.16	57

(*continued on next page*)

Appendix A (*continued*)

Depth (m)	Age (cal ka)	$CaCO_3$ (%)	TOC (%)	TN (%)	TS (%)	C/N ratio	C/S ratio	$\delta^{13}C_{org}$ (‰)	HI (mgHC/gC)
2.58	1.43	8.00	1.15	0.18	0.45	6.35	2.58	−20.96	51
2.70	1.49	8.29	1.11	0.19	0.48	5.80	2.30	−21.04	48
2.81	1.55	7.88	1.15	0.19	0.47	6.05	2.47	−21.05	48
2.92	1.61	7.99	1.14	0.19	0.51	6.04	2.24	−21.04	50
3.05	1.68	13.44	0.99	0.20	0.46	4.85	2.16	−21.41	58
3.18	1.72	8.55	1.04	0.20	0.43	5.16	2.39	−21.03	55
3.30	1.76	7.09	1.29	0.22	0.41	5.74	3.15	−21.00	49
3.39	1.79							−22.51	
3.42	1.80	6.83	1.34	0.23	0.47	5.78	2.83	−21.12	46
3.46	1.81	7.11	1.43	0.23		6.13		−21.79	84
3.52	1.83	7.52	1.17	0.23	0.50	5.10	2.36	−21.12	60
3.55	1.84	9.27	1.04	0.23	0.44	4.56	2.34	−21.16	56
3.62	1.86	8.75	1.21	0.25	0.43	4.92	2.83	−21.37	94
3.68	1.88	8.41	1.09	0.23	0.44	4.79	2.48	−21.45	61
3.71	1.89	8.72	1.09	0.25		4.40		−21.15	61
3.80	1.91	7.87	1.13	0.22	0.43	5.17	2.63	−21.25	56
3.82	1.92	8.79	1.10	0.29	0.45	3.77	2.47	−21.04	69
3.92	1.95	8.78	1.16	0.32	0.46	3.59	2.53	−21.17	77
4.02	1.98	8.12	1.19	0.30	0.47	3.91	2.54	−21.24	64
4.12	2.01	8.60	1.11	0.31	0.47	3.70	2.38	−21.51	64
4.22	2.04	7.93	1.16	0.29	0.53	3.84	2.18	−21.52	67
4.32	2.08	8.77	1.12	0.33	0.44	3.71	2.58	−21.36	71
4.42	2.11	7.53	1.21	0.31	0.52	3.58	2.35	−21.56	69
4.52	2.14	7.19	1.13	0.31	0.42	3.34	2.68	−21.84	61
4.61	2.17	8.10	1.05	0.36		3.67		−21.60	73
4.62	2.17	6.38	1.33	0.35	0.53	3.46	2.52	−22.13	52
4.72	2.20	7.17	1.20	0.35	0.43	3.80	2.81	−22.46	64
4.79	2.22	5.48	1.32	0.36	0.25	3.32	5.36	−22.32	58
4.96	2.27	8.41	1.18	0.12		10.66		−21.21	67
5.09	2.32	6.75	1.32		0.15		8.79	−21.45	53
5.25	2.40	8.97	1.07	0.15		7.03		−21.39	62
5.43	2.51	10.44	1.10	0.17	0.09	6.40	12.02	−22.01	68
5.60	2.60							−21.46	
5.77	2.70	10.71	1.01	0.17	0.08	5.94	12.92	−21.58	53
5.95	2.80	10.62	1.06	0.18		5.90		−21.39	64
6.12	2.89	10.72	1.10	0.19	0.42	5.90	2.60	−21.61	64
6.30	2.99	10.61	1.11	0.20	0.37	5.62	2.98	−21.74	73
6.42	3.06	8.77	1.17	0.20	0.38	5.89	3.10	−21.57	75
6.54	3.13	8.63	1.12	0.20	0.49	5.53	2.28	−21.40	73
6.67	3.20	8.98	1.14	0.22	0.50	5.14	2.27	−21.60	69
6.85	3.30	10.61	1.03	0.24	0.48	4.21	2.17	−21.67	69
7.02	3.40	8.21	1.30	0.27	0.35	4.79	3.70	−21.70	59
7.20	3.50	10.83	1.08	0.28	0.44	3.81	2.44	−21.55	61
7.37	3.59	8.05	1.33	0.28	0.33	4.80	4.07	−21.35	49
7.49	3.66	9.53	1.26	0.29		4.28		−21.40	50
7.61	3.73	9.76	1.20	0.31		3.87		−21.56	51
7.73	3.79	12.73	1.06	0.31		3.37		−21.33	60
7.85	3.86	10.84	1.14	0.34	0.42	3.39	2.74	−21.69	53
8.04	3.97	10.12	1.20	0.35	0.46	3.41	2.60	−21.67	64
8.32	4.12	9.40	1.06	0.36	0.41	2.92	2.60	−21.57	71
8.49	4.22	10.51	1.21	0.38		3.18		−21.39	49
8.62	4.29	9.33	1.25	0.35	0.72	3.54	1.74	−21.51	44

Appendix A (*continued*)

Depth (m)	Age (cal ka)	$CaCO_3$ (%)	TOC (%)	TN (%)	TS (%)	C/N ratio	C/S ratio	$\delta^{13}C_{org}$ (‰)	HI (mgHC/gC)
8.74	4.36	10.92	1.05	0.36		2.95		−21.22	56
8.87	4.43	11.41	1.04	0.39	0.44	2.68	2.35	−21.39	61
8.98	4.49	11.06	1.14	0.42	0.59	2.69	1.93	−21.52	69
9.10	4.56	11.32	1.12	0.43	0.44	2.63	2.56	−21.43	61
9.27	4.66	11.80	1.20		0.47		2.57	−21.36	76
9.39	4.72	9.67	1.41	0.09	0.44	15.63	3.20	−21.53	78
9.55	4.81	11.58	1.25	0.43		2.89		−21.40	77
9.67	4.88	10.49	1.22	0.49	0.43	2.49	2.83	−21.33	80
9.81	4.96	11.84	1.25	0.46	0.43	2.72	2.94	−22.13	97
9.97	5.05	11.87	1.22	0.48	0.45	2.53	2.69	−22.40	89
10.03	5.08	11.79	1.16	0.35		3.31		−21.76	72
10.19	5.12	11.68	1.21	0.45	0.42	2.70	2.86	−21.74	67
10.35	5.15	13.06	1.21	0.36	0.03	3.30	3.56	−22.32	95
10.50	5.18	11.38	1.18	0.45	0.43	2.62	2.73	−22.69	78
10.66	5.20	12.62	1.08	0.34		3.16		−22.13	
10.82	5.23	11.07	1.13	0.47	0.47	2.38	2.40	−21.90	
10.92	5.25	14.88	1.13	0.50	0.46	2.27	2.48	−21.94	
11.09	5.28	12.78	1.13	0.54	0.45	2.11	2.49	−21.65	
11.25	5.31	13.29	1.14	0.45	0.44	2.55	2.56	−21.68	
11.40	5.36	13.49	1.14	0.46	0.34	2.48	3.36	−21.79	
11.57	5.41	12.39	1.19	0.45	0.54	2.66	2.21	−21.96	
11.78	5.47	10.76	1.31	0.54	0.43	2.41	3.03	−21.94	
11.96	5.52	12.56	1.21	0.52	0.44	2.33	2.74	−22.19	
12.12	5.57	13.15	1.08	0.55	0.47	1.96	2.32	−22.11	
12.28	5.62	12.93	1.15	0.43	0.62	2.67	1.86	−21.92	
12.45	5.67	12.86	1.11	0.55	0.43	2.03	2.61	−22.43	
12.60	5.72	13.17	1.08	0.14	0.49	7.66	2.18	−22.20	
12.77	5.77	14.88	0.98	0.13	0.20	7.35	4.89	−21.95	
12.92	5.82	15.65	0.95	0.13	0.50	7.25	1.89	−22.12	
13.08	5.86	15.73	0.91	0.13	0.51	7.17	1.77	−22.39	81
13.22	5.91	15.47	1.13	0.14	0.46	7.91	2.45	−22.48	106
13.28	5.92	11.92	1.24	0.14	0.48	9.11	2.59	−22.42	68
13.40	5.96	12.87	1.22	0.13	0.49	9.30	2.48	−22.05	69
13.56	6.01	13.82	1.13	0.12	0.49	9.07	2.31	−22.23	66
13.73	6.06	14.16	1.03	0.12	0.52	8.35	1.98	−22.27	70
13.79	6.08	13.41	1.10	0.14	0.44	7.95	2.49	−21.95	70
13.89	6.11	14.99	0.87	0.14		6.44		−23.10	60
13.99	6.14	13.85	1.05	0.14	0.48	7.67	2.18	−22.23	84
14.01	6.14	16.39	0.74	0.09	0.41	8.30	1.82	−23.39	66
14.12	6.22	16.71	0.72	0.07	0.61	10.54	1.17	−23.39	96
14.14	6.23	17.04	0.43	0.07	0.02	6.02	22.52	−21.68	76
14.24	6.32	13.39	0.43	0.07	0.53	6.07	0.83	−23.40	53
14.29	6.36	12.22	0.29	0.06	0.42	5.33	0.70	−21.98	54
14.32	6.39	17.69	0.50	0.08	0.41	6.62	1.23	−22.83	67
14.39	6.45	15.06	0.43	0.06	0.02	7.35	23.51	−22.36	60
14.44	6.49	10.22	0.21	0.04		4.91		−22.19	44
14.47	6.52	14.76	0.36	0.06	0.01	5.89	33.70	−21.23	64
14.58	6.61	14.75	0.33	0.06	0.02	5.14	13.83	−21.42	73
14.59	6.62	7.96	0.30	0.05	0.01	6.70	26.11	−22.67	50
14.67	6.69	13.73	0.30	0.05	0.03	5.61	11.57	−22.35	51
14.76	6.77	9.12	0.18	0.03	0.18	6.47	1.01	−22.22	17

(*continued on next page*)

Appendix A (*continued*)

Depth (m)	Age (cal ka)	$CaCO_3$ (%)	TOC (%)	TN (%)	TS (%)	C/N ratio	C/S ratio	$\delta^{13}C_{org}$ (‰)	HI (mgHC/gC)
14.78	6.79	16.27	0.23	0.05	0.22	4.65	1.07	−22.37	65
14.84	6.84	7.67	0.24	0.03	0.15	7.10	1.59	−24.43	29
14.89	6.88	11.82	0.35	0.04	0.24	8.42	1.48	−22.64	34
14.93	6.92	7.06	0.28	0.04	0.18	7.57	1.58	−23.16	43
15.02	6.99	11.81	0.44	0.05	0.38	8.86	1.16	−24.72	45
15.11	7.07	3.20	0.58	0.08	0.36	7.06	1.63	−24.66	31
15.18	7.13	4.51	0.66	0.06	0.47	11.18	1.39	−24.81	38
15.29	7.23	3.46	0.74	0.06	0.56	12.94	1.33	−24.71	30
15.41	7.33	2.62	0.72	0.06	0.68	11.15	1.06	−24.99	45
16.23	8.04	5.82	0.69	0.07	0.59	10.63	1.18	−24.47	42
16.41	8.15	5.93	0.62	0.06	0.55	10.95	1.13	−24.72	39
16.58	8.25	4.30	0.59	0.06	0.65	9.73	0.92	−24.72	37
16.72	8.34	2.82	0.70	0.06	0.71	11.29	0.99	−24.83	37
16.86	8.43	3.28	0.74	0.07	0.59	10.39	1.27	−24.59	46
17.00	8.52	2.53	0.79	0.06	0.57	12.65	1.39	−25.16	51
17.14	8.60	2.39	0.78	0.08		10.34		−25.03	47
17.27	8.68	2.98	0.60	0.06	0.77	10.29	0.78	−24.89	43
17.41	8.77	0.97	0.94	0.08	0.72	12.49	1.32	−25.02	48
17.56	8.86	1.21	0.97	0.07		13.68		−25.06	36
17.80	9.01	2.19	0.72	0.07	0.81	10.98	0.89	−24.99	37
17.94	9.10	2.42	0.75	0.07	1.05	10.83	0.72	−25.06	36
18.08	9.19	1.06	0.94	0.07	0.67	13.12	1.41	−24.99	38
18.21	9.27	2.83	0.83	0.07	1.07	11.28	0.78	−25.45	53
18.36	9.36	5.11	0.80	0.08	1.31	10.52	0.61	−25.23	44
18.51	9.46	1.51	0.80	0.07		11.41		−25.04	37
18.66	9.55	2.67	0.60	0.06	0.65	10.44	0.93	−25.18	43
18.81	9.64	3.14	0.61	0.07	0.59	9.12	1.05	−24.66	43
18.95	9.73	3.53	0.67	0.07	0.49	9.62	1.37	−25.39	46
19.09	9.82	3.14	0.71	0.07	0.57	9.64	1.24	−25.18	48
19.23	9.90	4.33	0.64	0.07	0.72	8.76	0.89	−24.92	45
19.41	10.02	1.19	1.11	0.02	0.35	70.85	3.14	−25.67	59
19.53	10.09	2.24	0.70	0.06	0.62	11.20	1.12	−25.22	68
19.60	10.13	1.13	0.68	0.05	0.42	13.63	1.60	−24.75	25
19.66	10.17	1.66	0.78	0.06	0.54	12.95	1.44	−25.16	36
19.73	10.21	0.70	0.65	0.05	0.34	13.82	1.90	−25.36	23
19.81	10.26	0.19	0.75	0.05	0.66	14.20	1.13	−25.21	32
19.91	10.33	4.76	0.50	0.04	0.40	14.20	1.25	−25.80	44
19.99	10.38	1.81	0.26	0.03	0.34	8.46	0.75	−25.51	71
21.11	11.07	0.24	1.09	0.08		13.62		−25.82	44
21.23	11.15	1.66	0.11	0.02	0.22	6.18	0.50	−26.43	127
21.76	11.48	2.50	0.70	0.07	0.92	9.87	0.76	−25.48	57
21.86	11.54			0.05	0.55	0.00	0.00	−25.54	
21.93	11.58			0.03	0.43	0.00	0.00	−26.65	
22.00	11.63	2.31	0.74	0.07	1.02	10.95	0.72	−26.11	73
22.08	11.68	2.22	0.89	0.08	1.17	10.73	0.76	−25.66	83
22.19	11.75	1.50	0.52	0.05	0.68	9.48	0.76	−25.66	71
22.82	12.14	1.96	0.49	0.07		6.60		−25.93	86
22.95	12.30	1.98	0.35	0.09	0.43	3.97	0.81	−25.70	66
23.07	12.85	1.95	1.08					−24.86	73
23.18	13.36	1.99	1.00	0.10	1.03	9.74	0.97	−25.06	81
23.29	13.87	3.76	0.24	0.12	0.45	1.98	0.55	−24.10	57

Appendix B. Lithological results of core SSDP 102

Depth (m)	Age (cal ka)	Clay (%)	Coarse fraction (%)
0.20	0.12	59.34	4.47
0.55	0.34	63.62	4.55
1.50	0.85	63.16	3.92
1.98	1.11	62.8	1.64
2.54	1.41	68.32	1.76
2.96	1.63	64.21	4.51
3.40	1.79	62.78	5.25
3.49	1.82	63.05	5.75
3.77	1.90	66.25	2.81
4.72	2.20	62.35	7.14
4.85	2.24	63.41	3.18
5.40	2.47	52.92	8.28
5.90	2.73	62.13	4.1
6.61	3.10	61.7	1.97
7.12	3.36	59.91	3.32
7.60	3.60	64.27	2.73
8.07	3.85	63.43	1.82
8.26	3.94	63.8	3.48
8.55	4.09	62.06	4.83
9.02	4.33	58.49	14.95
10.00	4.83	64.66	2.44
10.50	5.09	61.67	4.85
11.60	5.41	59.69	12.07
11.74	5.46	58.13	1.88
12.35	5.64	58.5	5.35
12.86	5.80	55.26	11.33
13.24	5.91	55.46	5.73
13.50	5.99	50.51	8.64
13.67	6.04	59.19	4.06
13.93	6.12	58.58	8.56
14.06	6.16	14.78	71.91
14.54	6.57	19.84	57.36
14.99	6.96	11.97	70.34
15.47	7.37	27.02	22.29
16.65	8.29	18.83	36.49
17.18	8.62	36.47	7.73
17.62	8.90	29.49	14.15
17.75	8.98	28.91	15.52
18.42	9.40	23.41	13.68
18.87	9.68	28.95	14.54
19.31	9.95	35.59	6.19
21.72	11.45	23.26	35.22
22.27	11.80	22	37.56
23.33	14.03	12.05	73

Appendix C. Organic geochemical results of core SSDP 105

Depth (m)	Age (cal ka)	$CaCO_3$ (%)	TOC (%)	TN (%)	TS (%)	C/N ratio	C/S ratio	$\delta^{13}C_{org}$ (‰)	HI (mgHC/gC)
0.04	0.18	14.32	2.10	0.27	0.65	7.93	3.21	−21.98	493
0.33	1.46	13.48	2.09	0.27	0.66	7.63	3.15	−22.17	256
0.63	2.66	13.42	1.98	0.27	0.62	7.24	3.21	−21.52	477

(*continued on next page*)

Appendix C (*continued*)

Depth (m)	Age (cal ka)	$CaCO_3$ (%)	TOC (%)	TN (%)	TS (%)	C/N ratio	C/S ratio	$\delta^{13}C_{org}$ (‰)	HI (mgHC/gC)
0.94	2.69	14.90	1.79	0.25	0.53	7.12	3.37	−21.8	201
1.23	2.72	13.80	1.97	0.25	0.55	7.76	3.61	−21.48	312
1.54	2.75	12.43	1.98	0.26	0.52	7.74	3.83	−21.55	538
1.84	2.78	14.67	1.85	0.25	0.59	7.29	3.13	−21.62	338
2.15	2.81	12.20	2.09	0.27	0.53	7.85	3.95	−22	261
2.45	2.84	13.27	2.12	0.26	0.52	8.20	4.07	−21.74	197
2.75	2.87	15.97	1.85	0.32	0.50	5.72	3.71	−21.76	266
3.03	2.90	11.88	2.18	0.27	0.49	8.03	4.43	−21.98	383
3.24	2.92	13.42	1.99	0.28	0.47	6.99	4.21	−21.59	329
3.43	2.94	9.39	2.55	0.26	0.49	9.66	5.23	−21.9	141
3.54	2.96	14.80	1.83	0.27	0.41	6.83	4.42	−21.64	196
3.94	3.00	13.57	1.91	0.26	0.50	7.24	3.85	−21.6	185
4.34	3.04	18.48	1.73	0.25	0.38	6.83	4.53	−21.56	209
4.74	3.08	14.17	1.95	0.28	0.52	6.97	3.75	−21.82	198
5.79	3.19	14.27	1.98	0.29	0.63	6.89	3.17	−21.53	128
6.19	3.23	14.15	1.92	0.27	0.47	7.09	4.05	−21.7	209
6.59	3.27	14.60	2.00	0.27	0.40	7.34	4.94	−21.59	203
6.98	3.31	12.85	2.09	0.28	0.42	7.45	5.01	−21.36	206
7.51	3.37	14.45	2.02	0.28	0.40	7.20	5.07	−22.24	252
7.91	3.41	16.04	1.83	0.28	0.38	6.54	4.79	−21.36	178
8.31	3.45	13.52	2.06	0.28	0.42	7.30	4.94	−21.79	200
8.71	3.49	11.63	2.15	0.28	0.35	7.68	6.14	−21.53	194
9.11	3.53	12.84	2.15	0.29	0.37	7.40	5.78	−21.72	215
10.64	3.69	16.32	1.89	0.29	0.35	6.61	5.34	−21.49	176
10.99	3.73	16.07	1.78	0.29	0.32	6.16	5.63	−21.52	158
11.39	3.78	14.74	1.81	0.28	0.40	6.47	4.54	−21.46	144
11.79	3.84	12.27	2.33	0.30	0.30	7.91	7.75	−21.42	168
12.25	3.90	12.61	2.12	0.29	0.30	7.43	7.20	−21.77	118
12.68	3.96	15.12	1.89	0.27	0.33	6.89	5.76	−21.28	110
13.13	4.03	16.23	2.01	0.28	0.29	7.08	7.05	−21.87	174
13.48	4.08	14.57	2.26	0.30	0.37	7.55	6.04	−22.32	227
13.84	4.13	16.61	2.09	0.29	0.36	7.23	5.74	−22.11	230
14.23	4.18	13.99	2.04	0.28	0.41	7.19	5.03	−21.16	117
14.78	4.26	13.91	2.07	0.29	0.44	7.17	4.66	−21.19	122
15.23	4.32	13.87	2.05	0.29	0.34	7.06	6.05	−21.46	140
15.73	4.39	12.85	2.32	0.29	0.36	7.96	6.45	−22.38	149
16.18	4.45	13.08	2.09	0.29	0.36	7.17	5.77	−21.35	114
16.57	4.51	13.58	2.21	0.29	0.33	7.58	6.65	−21.91	140
16.95	4.56	13.83	2.10	0.30	0.43	7.09	4.92	−21.84	188
17.35	4.62	12.17	2.33	0.33	0.45	6.99	5.21	−21.46	174
17.75	4.68	13.72	2.84	0.30	0.39	9.51	7.29	−23.22	352
18.46	4.78	13.17	2.00	0.30	0.36	6.75	5.58	−21.32	198
18.85	4.83	12.62	2.44	0.30	0.39	8.24	6.27	−22.38	234
19.26	4.89	12.22	2.32	0.30	0.36	7.82	6.40	−22.18	246
19.67	4.95	13.72	2.11	0.29	0.38	7.34	5.58	−21.4	217
20.67	5.21	13.67	2.09	0.29	0.35	7.12	5.98	−21.4	194
21.14	5.35	14.88	2.04	0.31	0.34	6.63	6.04	−21.41	200
21.59	5.48	15.03	2.10	0.31	0.35	6.71	6.00	−21.51	173
22.00	5.61	15.28	2.05	0.29	0.37	7.08	5.58	−21.68	218
22.14	5.65	12.24	2.35	0.30	0.47	7.85	4.98	−22.19	224
22.44	5.74	12.79	2.16	0.29	0.44	7.43	4.86	−21.5	151
22.84	5.86	16.43	2.10	0.28	0.40	7.44	5.26	−21.55	234
23.24	5.98	13.05	2.25	0.29	0.35	7.90	6.51	−21.52	139

Appendix C (*continued*)

Depth (m)	Age (cal ka)	$CaCO_3$ (%)	TOC (%)	TN (%)	TS (%)	C/N ratio	C/S ratio	$\delta^{13}C_{org}$ (‰)	HI (mgHC/gC)
23.74	6.13	15.24	2.12	0.27	0.42	7.81	5.10	−21.97	200
24.24	6.28	12.12	2.31	0.28	0.34	8.31	6.74	−21.53	213
24.61	6.39	13.07	2.41	0.30	0.41	8.08	5.86	−21.95	179
25.21	6.57	13.67	2.22	0.32	0.43	6.89	5.15	−21.47	215
25.61	6.69	13.06	2.11	0.29	0.51	7.35	4.17	−21.5	217
26.11	6.83	12.28	2.35	0.30	0.51	7.96	4.58	−22.2	235
26.96	7.09	13.72	2.09	0.28	0.44	7.46	4.73	−21.59	214
27.56	7.27	12.77	2.21	0.29	0.44	7.51	5.02	−21.49	152
28.06	7.42	13.31	2.06	0.28	0.51	7.33	4.01	−21.47	232
28.43	7.53	14.04	2.08	0.29	0.45	7.29	4.64	−21.37	143
28.89	7.67	14.02	2.06	0.28	0.49	7.29	4.18	−21.55	135
29.20	7.76	13.07	2.18	0.28	0.59	7.72	3.71	−21.82	172
29.72	7.91	18.28	1.42	0.19	0.27	7.51	5.22	−23.7	241
29.88	8.04	5.69	0.50	0.11	0.11	4.62	4.58	−22.43	100
30.23	8.33	6.05	0.38	0.12	0.12	3.24	3.19	−23.13	87
30.97	8.93	7.46	0.15	0.10	0.09	1.59	1.69	−23.74	52
31.28	9.18	2.65	0.54	0.11	0.33	4.96	1.63	−25.48	70
31.95	9.72	5.35	0.34	0.10	0.24	3.39	1.42	−25.46	74
32.42		0.70	0.22	0.12	0.38	1.85	0.58	−24.66	65
34.04		0.13	0.08	0.09	0.22	0.89	0.37	−27.35	133
35.82		0.30	0.11	0.08	0.28	1.40	0.40	−27.62	140
36.19		0.35	0.20	0.09	0.25	2.33	0.81	−26	131
36.94		0.26	0.30	0.09	0.26	3.30	1.16	−26.63	58
37.26		0.57	0.07	0.10	0.36	0.74	0.20	−27.2	100
38.31		0.60	0.07	0.11	0.38	0.70	0.20	−27.35	71
38.99		6.34	0.67	0.16	1.79	4.32	0.37	−27.24	64
39.16		1.97	0.27	0.09	0.86	2.89	0.32	−28.17	253
39.41		4.33	0.67	0.14	1.63	4.89	0.41	−26.85	86
39.69		12.92	0.44	0.13	3.85	3.28	0.11	−27.08	29
39.81		3.30	0.28	0.10	1.25	2.80	0.23	−27.55	29
40.31		2.56	0.09	0.09	0.94	0.95	0.09	−27.58	67
40.83		8.72	0.62	0.14	2.67	4.37	0.23	−27.1	81
41.13		1.97	0.07	0.09	0.79	0.76	0.09	−26.5	100
41.58		7.98	2.14	0.66	6.49	3.26	0.33	−27.36	194
41.70		8.74	2.73	0.23	0.46	11.88	5.99	−29.04	455
41.79		0.05	1.12	0.18	0.31	6.23	3.60	−28.71	296
41.88		0.18	0.44	0.17	0.34	2.64	1.29	−27.49	126
42.05		0.22	0.43	0.17	0.32	2.48	1.37	−27.41	108
42.21		0.96	0.83	0.18	0.14	4.64	5.77	−28.21	155
42.33		0.30	0.27	0.14	0.19	1.88	1.39	−27.22	113
42.51		0.30	0.34	0.16	0.43	2.13	0.79	−27.07	104
42.68		0.17	0.34	0.16	0.17	2.18	1.94	−26.82	128
42.83		0.73	0.29	0.13	0.05	2.30	5.25	−26.66	158
43.23		1.36	0.43	0.13	0.13	3.31	3.41	−25.57	131
43.68		1.72	0.45	0.13	0.07	3.41	6.20	−26.34	162
44.08		5.32	0.28	0.13	0.48	2.17	0.59	−25.96	75
44.48		1.63	0.40	0.13	0.05	3.07	7.61	−26.78	138
44.88		3.02	0.15	0.13	0.91	1.16	0.16	−27.46	163
45.41		1.97	0.32	0.13	0.09	2.49	3.57	−27.01	88
45.81		0.35	0.39	0.14	0.10	2.81	3.73	−26.79	72
46.19		0.12	1.18	0.17	0.20	7.15	5.90	−29.01	311
46.56		0.20	0.51	0.15	0.16	3.43	3.14	−26.92	96
46.81		0.77	0.48	0.15	0.07	3.15	7.09	−27.2	78

(*continued on next page*)

Appendix C (*continued*)

Depth (m)	Age (cal ka)	$CaCO_3$ (%)	TOC (%)	TN (%)	TS (%)	C/N ratio	C/S ratio	$\delta^{13}C_{org}$ (‰)	HI (mgHC/gC)
47.21		0.74	0.54	0.15	0.11	3.60	4.87	−27.31	109
47.61		3.91	0.82	0.15	0.24	5.59	3.44	−27.73	85
48.01		1.73	0.65	0.14	0.18	4.52	3.57	−27.48	85
48.13		0.73	0.58	0.14	0.36	4.07	1.60	−26.85	70
48.51		0.83	0.62	0.15	0.22	4.20	2.85	−26.86	114
48.92		0.30	0.49	0.15	0.26	3.28	1.85	−26.68	94
49.07		1.96	0.58	0.15	0.80	3.75	0.72	−26.65	112
49.43		3.17	0.84	0.16	0.86	5.34	0.98	−27.46	89
49.83		1.73	0.57	0.16	0.28	3.57	2.03	−27.82	113

Appendix D. Lithological results of core SSDP 105

Depth (m)	Age (cal ka)	Clay (%)	Coarse fraction (%)
1.00	2.69	59.13	2.26
3.35	2.94	52.98	2.06
4.92	3.10	51.91	5.62
7.05	3.32	56.86	3.95
9.08	3.53	61.85	1.68
11.62	3.81	50.44	7.00
13.87	4.13	59.58	0.88
15.75	4.39	7.90	0.26
17.94	4.70	51.82	3.53
19.89	4.98	53.68	5.61
21.93	5.58	54.36	1.38
24.27	6.28	50.74	3.66
26.38	6.92	53.79	3.18
28.33	7.50	45.19	9.36
28.91	7.67	52.22	10.20
29.36	7.81	50.44	7.00
29.79	7.86	9.78	76.24
30.07	8.14	5.51	87.50
30.26		6.98	84.85
30.95		3.07	39.93
31.46		11.00	59.68
31.91		9.97	76.86
32.4		9.16	73.39
34.01		5.24	82.53
35.81		6.06	87.24
36.17		9.22	80.71
37.16		5.88	85.47
37.24		7.45	82.62
37.47		14.26	67.00
38.53		17.25	67.07
39.14		8.45	76.98
39.39		24.47	46.21
40.08		7.92	77.44
40.34		10.86	74.51
40.71		38.74	23.29
41.14		6.95	86.53
41.39		6.05	84.38
43.02		44.25	14.79

Appendix D (*continued*)

Depth (m)	Age (cal ka)	Clay (%)	Coarse fraction (%)
43.22		43.23	15.69
43.42		44.31	14.56
43.84		57.04	9.83
45.06		37.09	20.31
46.28		56.16	0.12
46.53		52.45	0.33
47.8		8.11	5.32
47.97		8.16	1.85
48.16		3.17	83.08
48.89		8.51	1.20

References

Anderson, J.B., 1975. Factors controlling $CaCO_3$ dissolution in the Wedell Sea from foraminiferal distribution patterns. Marine Geology 19, 315–332.

Bard, E., Arnold, M., Hamelin, B., Laborde, N.T., Cabioch, G., 1998. Radiocarbon calibration by means of mass spectrometric $^{230}Th/^{234}U$ and ^{14}C ages of corals: an updated database including samples from Barbodos, Mururoa and Tahiti. Radiocarbon 40 (3), 1085–1092.

Berner, R.A., Raiswell, R., 1984. C/S method for distinguishing freshwater from marine sedimentary rocks. Geology 12, 365–368.

Be′, A.W.H., 1977. An ecological, zoogeographical and taxonomic Review of recent planktonic foraminifera. In: Ramsay, A.T.S. (Ed.), Oceanic Micropaleontology. Academic Press, London, p. 100.

Fairbanks, R.G., 1990. The age and origin of the Younger Dryas climate event in Greenland Ice cores. Paleoceanography 5 (6), 937–948.

Galehouse, J.S., 1971. Sedimentation analysis. In: Carver, R.E. (Ed.), Procedures in Sedimentary Petrology. Wiley-Interscience, New York, pp. 69–94.

Ijiri, A., Wang, L., Oba, T., Kawahata, H., Huang, C.-Y., Huang, C.-Y., 2005. Paleoenvironmental changes in the northern area of the East China Sea during the past 42,000 years. Palaeogeography, Palaeoclimatology, Palaeoecology 219, 239–261.

Jin, J.H., Chough, S.K., 1998. Partitioning of transgressive deposits in the SE Yellow Sea: a sequence stratigraphic interpretation. Marine Geology 149, 79–92.

Jian, Z., Wang, P., Saito, Y., Wang, J., Pflaumann, U., Oba, T., Cheng, X., 2000. Holocene variability of the Kuroshio Current in the Okinawa Trough, northwestern Pacific Ocean. Earth and Planetary Science Letters 184, 305–319.

Kawahata, H., Ohshima, H., Shimada, C., Oba, T., 2003. Terrestrial-oceanic environmental change in the southern Okhotsk Sea during the Holocene. Quaternary International 108, 67–76.

Keigwin, L.D., Gorbarenko, S.A., 1992. Sea level, surface salinity of the Japan Sea and the Younger Dryas event in the northwestern Pacific ocean. Quaternary Research 37, 346–360.

Kellogg, T.B., 1976. Late Quaternary climatic changes: evidence from deep-sea cores of Norwegian and Greenland Seas. In: Cline, R.M., Hays, J.D. (Eds.), Investigation of Late Quaternary Paleoceanography and Paleoclimatology. Geological Society of America Memoirs 145, 77–110.

Korea Institute of Geoscience and Mineral Resource (KIGAM), 2000. Study on Quaternary stratigraphy and environmental changes in Korean Sea. KIGAM Research Report KR-00(B)-02, 75–145.

Kim, D.C., Sung, J.Y., Park, S.C., Lee, G.H., Choi, J.H., Kim, G.Y., Seo, Y.K., Kim, J.C., 2001. Physical and acoustic properties of shelf sediments, the South Sea of Korea. Marine Geology 179, 39–50.

Knies, J., Stein, R., 1998. New aspects of organic carbon deposition and its paleoceanographic implications along the northern Barents Sea margin during the last 30,000 years. Paleoceanography 13, 384–394.

Lambeck, K., Yokoyama, Y., Purcell, T., 2002. Into and out of the Last Glacial Maximum: sea-level change during Oxygen Isotope Stages 3 and 2. Quaternary Science Reviews 21, 343–360.

Lee, E., Nam, S., 2003. Freshwater supply by Korean rivers to the East Sea during the last glacial maximum: a review and new evidence from the Korea Strait region. Geo-Marine Letters 23, 1–6.

Liu, J.P., Milliman, J.D., Gao, S., Cheng, P., 2004. Holoecene development of the Yellow River's subaqueous delta, North Yellow Sea. Marine Geology 209, 45–67.

Min, G.H., 1994. Seismic stratigraphy and depositional history of Pliocene–Holocene deposits in the southeastern shelf of the Korean Peninsula. Ph.D. Thesis, Seoul National University Seoul, Korea, p. 196.

Oba, T., Kato, M., Kitazato, H., Omura, A., Sakai, T., Takayama, T., 1991. Paleoenvironmental changes in the Japan Sea during the last 85,000 years. Paleoceanography 6 (4), 499–518.

Park, B.K., Khim, B.K., 1990. Clay minerals of the recent fine-grained sediments on the Korean continental shelves. Continental Shelf Research 12, 1179–1191.

Park, S.C., Chu, K.S., 1991. Dispersal pattern of river-derived fine-grained sediment on the inner shelf of the Korea Strait. In: Takano, K. (Ed.), Oceanography of Asian Marginal Sea, 54. Elsevier Oceanography Series, pp. 231–240.

Park, S.C., Hong, S.K., Kim, D.C., 1996. Evolution of late Quaternary deposits on the inner shelf of the South Sea of Korea. Marine Geology 131, 219–232.

Park, S.C., Yoo, D.G., 1988. Depositional history of Quaternary sediments on the continental shelf off southeastern coast of Korea (Korea Strait). Marine Geology 79, 65–75.

Park, S.C., Yoo, D.G., Lee, K.-W., Lee, H.-H., 1999. Accumulation of recent muds associated with coastal circulations, southeastern Korea Sea (Korea Strait). Continental Shelf Research 19, 589–608.

Park, S.C., Yoo, D.G., Lee, C.-W., Lee, E.I., 2000. Last glacial sea-level changes and paleogeography of the Korea (Tsushima) Strait. Geo-Marine Letters 20, 64–71.

Qin, Y., Chen, L., Zhao, Y., Zhao, S., 1996. Geology of the East China Sea. Science Press, Beijing, pp. 139–151.

Ruttenberg, K.C., Goñi, M.A., 1997. Phosphorus distribution, C:N:P ratios, and $\delta^{13}C_{oc}$ in arctic, temperate, and tropical coastal sediments: tools for characterizing bulk sedimentary organic matter. Marine Geology 139, 123–145.

Suk, B.C., 1989. Quaternary sedimentation processes, structures and sea level changes in the East China Sea, the Yellow Sea and the Korea-Tsushima Strait regions. Ph.D. thesis, University of Tokyo, Tokyo, Japan, p. 246.

Stein, R., 1991. Accumulation of organic carbon in marine sediments. Lecture Notes in Earth Sciences 34, Springer, Heidelberg, p. 30–31.

Stein, R., Schubert, C., Vogt, C., Fterer, D., 1994. Stable isotope stratigraphy, sedimentation rates, and Salinity changes in the Latest Pleistocene to Holocene eastern central Arctic Ocean. Marine Geology 119, 335–355.

Steinsund, P.I., Hald, M., 1994. Recent calcium carbonate dissolution in the Barents Sea: paleoceanographic applications. Marine Geology 117, 303–316.

Tissot, B.P., Welte, D.H., 1984. Petroleum Formation and Occurrence. Springer-Verlag, Berlin, p. 699.

Wang, P., Min, Q., Bian, Y., 1985. On marine-Continental Transitional Faunas in Cenozoic Deposits of East China. China Ocean Press, Beijing, pp. 15–33.

Xu, X., Oda, M., 1999. Surface-water evolution of the eastern East China Sea during the last 36,000 years. Marine Geology 156, 285–304.

Yoo, D.G., Park, S.C., 1997. Late Quaternary prograding lowstand wedges on the shelf margin and trough region of the Korea Strait. Sedimentary Geology 109, 121–133.

Yoo, D.G., Park, S.C., 2000. High-resolution seismic study as a tool for sequence stratigraphic evidence of high-frequency sea-level changes: latest Pleistocene–Holocene example from the Korea Strait shelf. Journal of Sedimentary Research 70, 296–309.

Yoo, D.G., Park, S.C., Don, S., Oh, J.-H., 2003. Evolution and chronology of late Pleistocene shelf-perched lowstand wedges in the Korea Strait. Journal of Asian Earth Sciences 22, 29–39.